Electronic Supplementary Material (ESI) for Catalysis Science & Technology.

Facile Synthesis of Self-Supported Amorphous Phosphorus doped $Ni(OH)_2$ Composite Anodes for Efficient Water Oxidation

Gang Yuan, [a,b] *Yujie Hu,* [a] *Zihan Wang,* [a] *Qiwei Wang,* [a] *Li Wang,* [a,b] *Xiangwen Zhang,* [a,b] *Qingfa Wang* [a,b,*]

Corresponding Author

[*] E-mail：qfwang@tju.edu.cn

[a] Key Laboratory for Green Chemical Technology of the Ministry of Education, School of Chemical Engineering and Technology, Tianjin University, 92 Weijin Road, Tianjin 300072, P. R. China.

[b] Collaborative Innovation Centre of Chemical Science and Engineering (Tianjin), Tianjin University, Tianjin 300072, P. R. China.

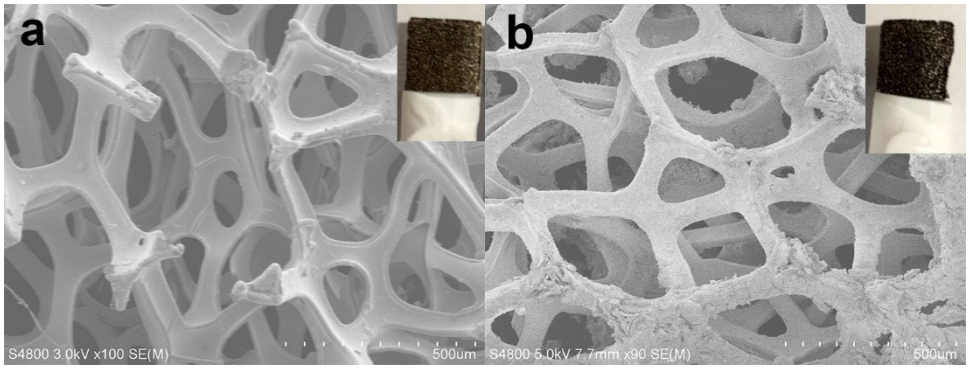

Fig. S1. SEM images of (a) bare NF, and (b) Ni-OH/P. The insets are the corresponding bulk sample.

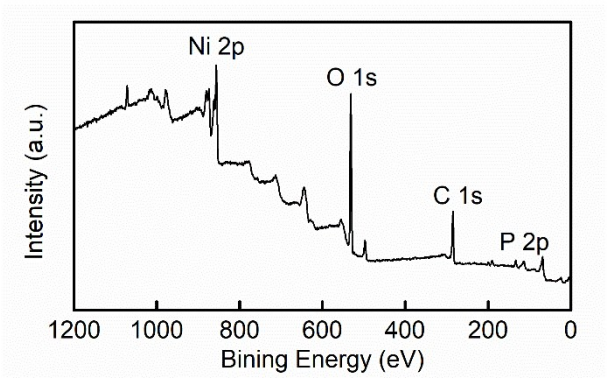

Fig. S2 XPS survey spectrum of Ni-OH/P.

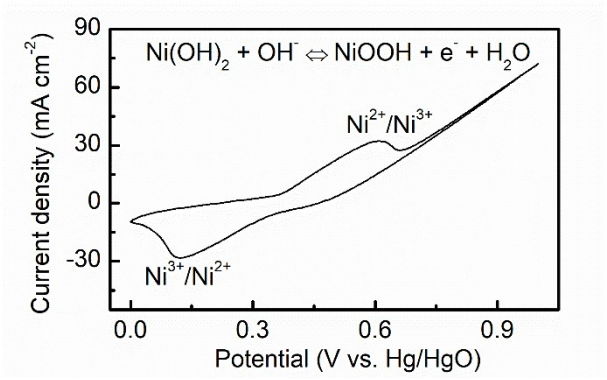

Fig. S3 Cyclic voltammogram of Ni-OH/P recorded in 1.0 M KOH at a scan rate of 50 mV/s.

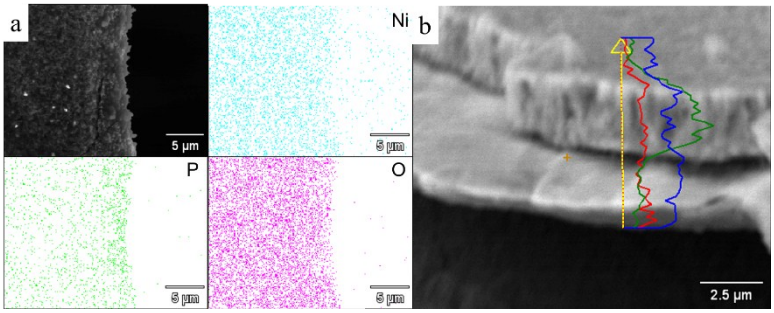

Fig. S4 EDS (a) elemental mapping of Ni-OH/P and (b) the elemental linear scan of P (green

line), O (red line), and Ni (blue line) in Ni-OH/P at its cross-sectional view.

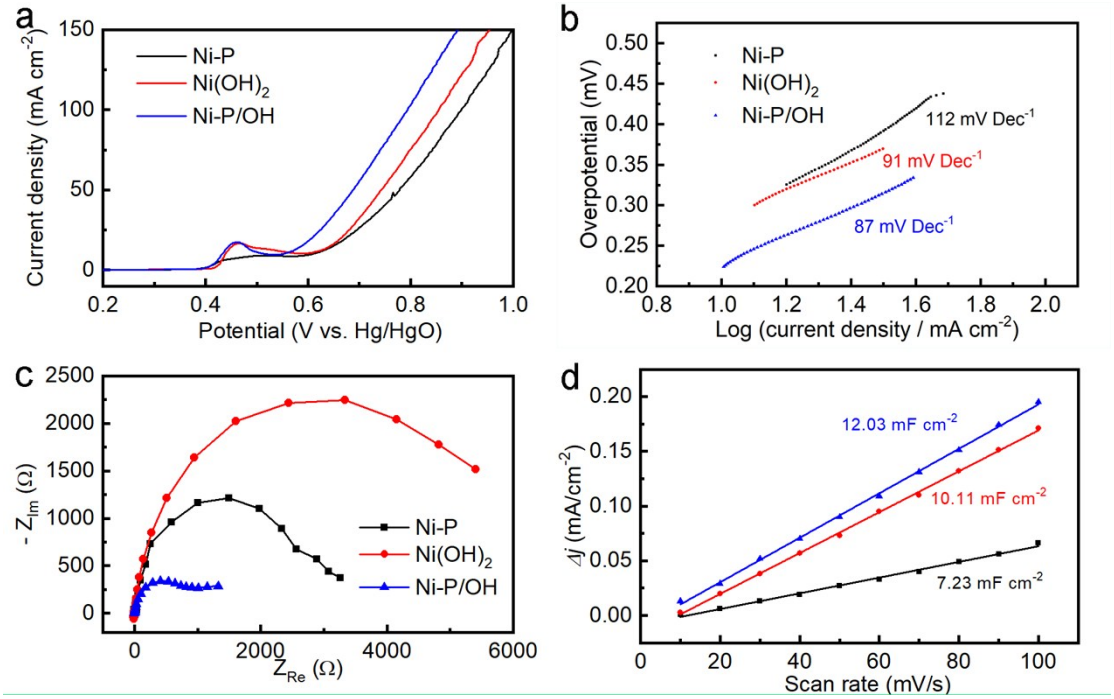

Fig. S5 (a) LSV, (b) Tafel, (c) C_{dl}, and (d) EIS plots of Ni-P, $Ni(OH)_2$, and Ni-OH/P. Reaction solution: 1.0 M KOH; Scan rate: 2 mV/s; EIS from 100 kHz to 10 mHz. The differences in current density variation (Δj=ja-jc) at -0.80 V plotted against scan rate fitted to a linear regression enables the estimation of Cdl value of Ni-OH/P.

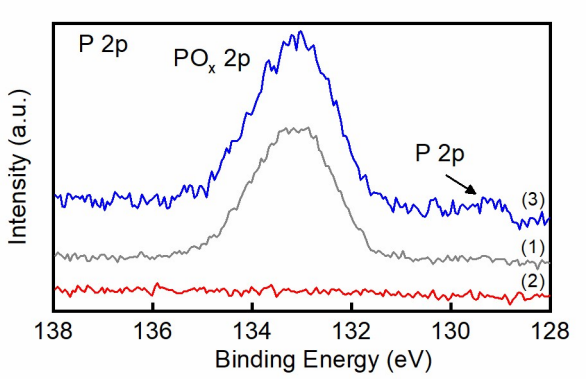

Fig. S6. High-resolution P 2p spectrum from (1) Ni phosphate, (2) $Ni(OH)_2$, and (3) Ni-OH/P, which were synthesized by hydrothermal treating NF in the solution of NaOAc, NaH_2PO_2, and NaOAc and NaH_2PO_2, respectively.

The high-resolution P 2p spectrum from various catalysts were provided in Figure S6.[1] The NiP_x species were formed when both NaOAc and NaH_2PO_2 were added in the hydrothermal solutions. In control experiments, only $Ni(OH)_2$ or Ni phosphate species were formed in the surface of Ni foam when only NaOAc or NaH_2PO_2 were added in the solutions, respectively. It indicates that NiP_x species can be generated with the help of both NaOAc and NaH_2PO_2. The above results confirm the existence of $Ni(OH)_2$ and Ni phosphide (NiP_x) in the catalyst. We have added the above-mentioned results in the revised manuscript.

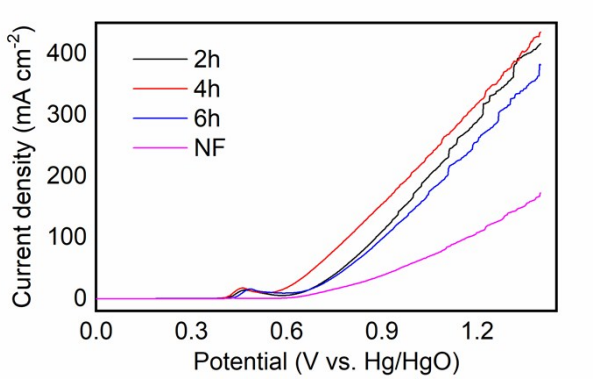

Fig. S7. LSV plots of bare NF and Ni-OH/P samples prepared with a duration at 2h, 4h, and 6h in 1.0 M KOH with a scan rate of 2 mV/s.

We have prepared three samples by adjusting the hydrothermal duration for 2h, 4h, and 6h. Their OER activities were tested by LSV, as in Figure R7. It can be seen that the sample prepared with a duration of 4h exhibits the highest OER activity. This result is similar to that from our previous work [2], where we have demonstrated that the self-supported core-shell Ni foam-catalyst composite anode has the highest activity when the shell is not too thin or too thick, because a long-time hydrothermal treatment is good for the growth of a thick layer of catalyst, while the conductivity of metallic NF is better than the catalyst layer. Hence, the promising catalyst design for OER should balance activity and conductivity by harmonizing the individual advantages of catalyst shell and metallic core. We have included these results in the revised supporting information.

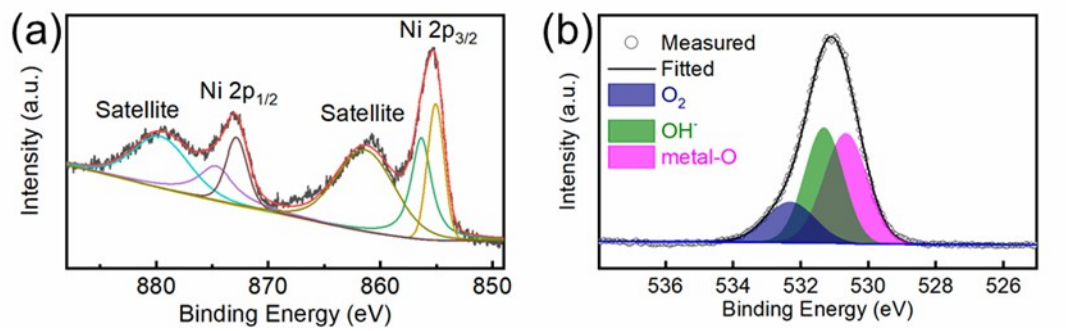

Fig. S8. High resolution (a) Ni 2p and (b) O 1s XPS spectra of post-run Ni-OH/P.

The more detailed metal valence and oxidation state of the post-run Ni-OH/P catalyst were further characterized by XPS measurements and the corresponding results are presented in Figure S8. In the high-resolution Ni 2p spectra (Figure S8a), two types of nickel species containing Ni^{2+} and Ni^{3+} were observed. The fitting peaks at 856.3 eV and 874.8 eV can be assigned to Ni^{3+}, while the fitting peaks at 855.0 eV and 872.9 eV are corresponding to Ni^{2+}.[3, 4] The satellite peaks at near 861.5 eV and 879.7 eV are two shake-up type peaks of nickel at the high binding energy side of the Ni $2p_{3/2}$ and Ni $2p_{1/2}$ edge. The electron couple of Ni^{3+}/Ni^{2+} indicating the existence of $Ni(OH)_2$ and NiOOH in the composite. The high-resolution spectrum for the O 1s region (Figure S8b) were fitted into three oxygen contributions. The peak locating at 530.7 eV is typical metal–oxygen bonds of NiOOH.[5] The peak at 531.3 eV is usually associated with oxygen in OH^- groups.[6] The peak at 532.3 eV can be attributed to adsorbed water or possibly adsorbed O_2.[7]

Table S1 Comparisons of different self-supported Ni-based OER catalysts in alkaline solution (1M KOH).

Catalyst	Substrate	Loading mass (mg cm^{-2})	η_{10} (mV)	η_{50} (mV)	η_{100} (mV)	Tafel slope (mV dec^{-1})	Ref.
Ni-OH/P	Ni foam	2.25	195	384	490	87	This work
NiFeSP	Ni foam	4.2		240		76.3	[8]
CoFe-LDH	Ni foam	1.2	274			-	[9]
NiFe LDH	Ni foam	8.3	244			32	[10]
CS-NiFeCu	Ni foam	1.6	180			33	[11]
NiFe LDH/r-GO	Ni foam	0.25	210			42	[12]
AN-NiFe	Ni foam	0.1	254			63	[13]
NiNH	Ni foam	4.9	231			81	[14]
α-NiOOH	Ni foam	0.74	266	350		76.3	[15]
NiO	Ni foam	0.5	345	410		53	[16]
NiFe-OH	Ni foam	-	215			32	[17]
FeNi LDH	Ni foam	-	227			38	[18]
FeNi-O	Ni foam	-	213			32	[18]

Reference

1. G. Yuan, Y. Hu, Q. Wang, Z. Wang, L. Wang, X. Zhang and Q. Wang, *Inorganic Chemistry Frontiers*, 2019, **6**, 3093-3096.
2. G. Yuan, X. Niu, Z. Chen, L. Wang, X. Zhang and Q. Wang, *ChemElectroChem*, 2018, **5**, 2376-2382.
3. J.-G. Kim, D. Pugmire, D. Battaglia and M. Langell, *Applied surface science*, 2000, **165**, 70-84.
4. A. Carley, S. Jackson, J. O'shea and M. Roberts, *Surface science*, 1999, **440**, L868-L874.
5. A. Mansour and C. Melendres, *Surface Science Spectra*, 1994, **3**, 271-278.
6. D. Cappus, C. Xu, D. Ehrlich, B. Dillmann, C. Ventrice Jr, K. Al Shamery, H. Kuhlenbeck and H.-J. Freund, *Chemical Physics*, 1993, **177**, 533-546.

7. Y. E. Roginskaya, O. Morozova, E. Lubnin, Y. E. Ulitina, G. Lopukhova and S. Trasatti, *Langmuir : the ACS journal of surfaces and colloids*, 1997, **13**, 4621-4627.
8. Y. Xin, X. Kan, L.-Y. Gan and Z. Zhang, *ACS Nano*, 2017, **11**, 10303-10312.
9. L. Han, C. Dong, C. Zhang, Y. Gao, J. Zhang, H. Gao, Y. Wang and Z. Zhang, *Nanoscale*, 2017, **9**, 16467-16475.
10. X. Xu, F. Song and X. Hu, *Nature communications*, 2016, **7**, 12324.
11. P. Zhang, L. Li, D. Nordlund, H. Chen, L. Fan, B. Zhang, X. Sheng, Q. Daniel and L. Sun, *Nature communications*, 2018, **9**, 381.
12. C. C. McCrory, S. Jung, I. M. Ferrer, S. M. Chatman, J. C. Peters and T. F. Jaramillo, *Journal of the American Chemical Society*, 2015, **137**, 4347-4357.
13. Z. Cai, L. Li, Y. Zhang, Z. Yang, J. Yang, Y. Guo and L. Guo, *Angew Chem Int Ed Engl*, 2019, **58**, 4189-4194.
14. Y. Ma, J. Chu, Z. Li, D. Rakov, X. Han, Y. Du, B. Song and P. Xu, *Small*, 2018, **14**, e1803783.
15. Q. Zhang, C. Zhang, J. Liang, P. Yin and Y. Tian, *ACS Sustainable Chemistry & Engineering*, 2017, **5**, 3808-3818.
16. J. Liang, Y.-Z. Wang, C.-C. Wang and S.-Y. Lu, *Journal of Materials Chemistry A*, 2016, **4**, 9797-9806.
17. X. Lu and C. Zhao, *Nature communications*, 2015, **6**, 6616.
18. X. Long, Z. Ma, H. Yu, X. Gao, X. Pan, X. Chen, S. Yang and Z. Yi, *Journal of Materials Chemistry A*, 2016, **4**, 14939-14943.